Enone− and Chalcone−Chloroquinoline Hybrid Analogues: In Silico Guided Design, Synthesis, Antiplasmodial Activity, in Vitro Metabolism, and Mechanistic Studies

ARTICLE *in* JOURNAL OF MEDICINAL CHEMISTRY · MAY 2011

Impact Factor: 5.45 · DOI: 10.1021/jm200149e · Source: PubMed

Published in final edited form as:
J Med Chem. 2011 May 26; 54(10): 3637–3649. doi:10.1021/jm200149e.

Enone- and chalcone-chloroquinoline hybrid analogs: *In silico*-guided design, synthesis, antiplasmodial activity, *in vitro* metabolism and mechanistic studies

Eric M. Guantai[a,b], **Kanyile Ncokazi**[a], **Timothy J. Egan**[a], **Jiri Gut**[c], **Philip J. Rosenthal**[c], **Ravi Bhampidipati**[d], **Anitha Kopinathan**[d], **Peter J. Smith**[b], and **Kelly Chibale**[a,e,*]

[a]Department of Chemistry, University of Cape Town, Rondebosch 7701, South Africa

[b]Division of Pharmacology, University of Cape Town, Observatory 7925, South Africa

[c]Department of Medicine, San Francisco General Hospital, University of California at San Francisco, CA 94143, USA

[d]Centre for Drug Candidate Optimisation, Monash Institute of Pharmaceutical Sciences, Monash University (Parkville campus), 381 Royal Parade, Parkville, VIC 3052, Australia

[e]Institute of Infectious Disease and Molecular Medicine, University of Cape Town, Rondebosch 7701, South Africa

Abstract

Analogs of the previously reported antimalarial hybrid compounds **8b** and **12** were proposed with the aim of identifying compounds with improved solubility and retained antimalarial potency. *In silico* characterization predicted improved solubilities of the analogs, particularly at low pH; they retained acceptable predicted permeability properties, but were predicted to be susceptible to hepatic metabolism. These analogs were synthesized and found to exhibit notable *in vitro* antimalarial activity. Compounds **25** and **27** were the most active of the analogs. *In vitro* metabolism studies indicated susceptibility of the analogs to hepatic metabolism. There was also evidence of primary glucuronidation for analogs **24** – **27**. Presumed *cis* - *trans* isomerism of **12, 22** and **23** under *in vitro* metabolism assay conditions was also observed, with differences in the nature and rates of metabolism observed between isomers. Biochemical studies strongly suggested that inhibition of hemozoin formation is the primary mechanism of action of these analogs.

Introduction

The World Health Organization (WHO) estimates that over 200 million episodes of malaria occur annually.[1;2] These result in between 0.6 – 1.2 million deaths a year, nearly all caused by *Plasmodium falciparum*, with ~85% of these deaths being of children below the age of 5 years in sub-Saharan Africa.[1] *P. falciparum*, the most virulent species of the malaria parasite, has developed varying degrees of resistance to many classes of drugs,[3;4] including possibly artemisinin-derived antimalarials.[5;6] Thus, the development of new, highly efficacious drugs to treat malaria remains a key priority.[7]

Antimalarial drug discovery, and indeed drug discovery in general, faces a myriad of challenges. For example, it is widely acknowledged that challenging physicochemical and absorption, distribution, metabolism and excretion (ADME) properties significantly hamper the development of many promising compounds into leads and drug candidates.[8;9] This has

*Corresponding author: Kelly.Chibale@uct.ac.za Tel: +27 21 650 2553 Fax: +27 21 650 5195.

led to an increased interest in the early determination (and/or prediction) of ADME properties, with simultaneous filtering *in vitro* for potency.[8;10] The use of large compound and data sets has dramatically increased the ability to model biological processes and relate these to easily measured or calculated physicochemical and structural features of the compounds.[11;12] *In silico* (computational) ADME prediction models and tools therefore complement *in vitro* and *in vivo* ADME experiments by facilitating the characterization of compounds prior to their synthesis,[9;11] thereby focusing synthetic and experimental evaluation efforts on a smaller number of particularly promising compounds. However, the results from such predictions should, whenever possible, be corroborated by *in vitro* and/or *in vivo* ADME assays.

For drugs to treat uncomplicated malaria, oral administration is practically mandatory, as huge numbers of patients across the developing world must be treated in facilities with limited resources or infrastructure.[10;13] The proportion of an orally administered drug that is delivered into the systemic circulation (i.e. its oral bioavailability) is heavily dependent on three primary factors: solubility, permeability and metabolic stability.[14;15] The *in silico* prediction and/or *in vitro* determination of these three factors is therefore highly valuable in antimalarial drug design.

In this study, *in silico* prediction tools were applied in the characterization of a series of analogs proposed for synthesis. These analogs were based on the promising antimalarial chalconechloroquinoline hybrid compound **8b** and the lower molecular weight intermediate **12**) (Figure 1), both of which were identified and reported previously.[16] One of the main concerns about compound **8b** was its poor aqueous solubility, which necessitated the use of up to 10% DMSO as co-solvent and extended periods of sonication and agitation during the initial dissolution of the compounds in the preparation of the stock solutions for *in vitro* evaluation. The compound was thus anticipated to have poor oral bioavailability.

The core structural features thought to be responsible for the observed antimalarial activity of **8b** and **12**, and which were therefore to be retained in the analogs, were identified as the chloroquinoline moiety and either the phenyl-butenone moiety (for **12**) or the chalcone moiety (for **8b**) (Figure 1) - the chloroquinoline moiety for its role in inhibition of hemozoin formation,[17] and the chalcone and phenyl-butenone moieties for their possible dual roles in malarial cysteine protease inhibition[18] and facilitating inhibition of hemozoin formation through π-π stacking interactions.

A small series of analogs of **8b** and **12** was therefore proposed based on the replacement of the triazole linker. These proposed analogs **20** – **27** (Figure 2) contained amino-alkyl or piperazinyl-based linkers, thereby introducing the 4-amino-substitution on the chloroquinoline sub-unit and resulting in more polar compounds with potentially enhanced (pH-dependent) solubility. In addition, the piperazinyl-based linkers possess an additional protonatable nitrogen, which should further enhance the ionization of the analogs bearing this type of linker. Analogous features are present in chloroquine and amodiaquine, both of which are established chloroquinoline antimalarials that possess a 4-amino substitution and a second protonatable nitrogen, and which have been successfully formulated as water-soluble salts.

The *in silico* characterization of the proposed analogs and their subsequent synthesis and biological evaluation is reported and discussed herein.

Results and discussion

In silico characterization of 8b, 12 and the proposed analogs

Three software packages, with varying but complementary capabilities, were applied for the *in silico* prediction of various parameters of interest. VolSurf+ was applied to predict physicochemical and ADME parameters of the compounds, such as aqueous solubility (at various pHs), Caco2 permeability and metabolic stability.[19;20] MetaSite was applied to predict sites of metabolism by hepatic cytochrome P450 enzymes and the structures of possible metabolites.[21;22] MoKa was used to predict the pKa of ionizable compounds.[23] These three software packages are available from Molecular Discovery (http://www.moldiscovery.com/software.php).

The chloroquinoline-based antimalarials chloroquine and amodiaquine were selected as reference compounds and were characterized with and compared to the study compounds. A deliberate attempt was made not to over-interpret the prediction results, but rather to use them as a guide in determining whether or not the proposed compounds were likely to be improvements on the parent compounds **8b** and **12**, and to highlight any potential liabilities.

Figure 3A shows the logarithm of the predicted aqueous solubility (log Sol.) plotted against the predicted n-Octanol-water partition coefficient (logD) at approximately physiological pH (pH 7.5) and at pH 5.0 for the compounds of interest. Chloroquine and amodiaquine showed significantly superior predicted aqueous solubility at both pHs when compared to **8b**, **12** and the proposed analogs. At both pH 5.0 and 7.5, **8b** showed the lowest predicted solubility; **12** was predicted to be more soluble than **8b**, most likely due to its lower molecular weight. As expected, a similar trend was seen for the proposed compounds, whereby analogs of **12** were predicted to be more soluble than the corresponding analogs of **8b**.

At pH 7.5, the predicted solubilities of the proposed analogs were only slightly higher than those of the parent compounds. However, as anticipated, there was a significant influence of pH on the predicted solubilities, which were significantly higher at pH 5.0 than 7.5. This difference is attributable to the fact that these basic compounds would exist predominantly in their ionized state at lower pH levels, rendering them more soluble. Analysis with MoKa predicted that compounds 20 – 27 were >90% ionized at pH 5.0.

The number of protonatable centers was also predicted to influence pH-dependent solubility. For example, among the analogs of **12**, the piperazinyl analogs **22, 24** and **26** (which have two protonatable centers) had higher predicted solubilities at pH 5.0 than the amino-ethoxy analog **20**, despite the fact that these three piperazinyl derivatives have higher molecular weights than **20**. A similar trend was observed for the analogs of **8b**, and both observations can be attributed to the positive influence on solubility of the higher charge-to-mass ratio afforded by the di-protonation of the piperazinyl analogs.

Prediction of Caco2 permeability was qualitative. When projected onto the two-dimensional PLS plot of the database of compounds used to generate the Caco2 permeation model, all the compounds (along with chloroquine and amodiaquine) showed acceptable predicted Caco2 permeation, falling within the blue (permeable) zone of the plot (Figure 3B).

Amodiaquine and chloroquine were predicted to have intermediate metabolic stability, falling somewhat between the blue (stable) and red (unstable) zones on the PLS plot (Figure 3B); they were predicted to be more stable to metabolism than the test compounds. **8b** was predicted to be less stable to hepatic metabolism than **12**. The proposed analogs were also shown to have relatively low predicted metabolic stabilities, particularly compounds **22, 23**

and **27**. Site-of-metabolism analysis was carried out on MetaSite in an attempt to shed light on these findings (Figure 4).

The main route of metabolism for **8b** was predicted to be O-demethylation of the *para*-methoxy group on ring B, as indicated by the blue ring highlighting this group; this group is absent in **12**. O-demethylation on ring A and N-oxidation of the quinoline ring were the main routes of metabolism predicted for **12**, but these may not be as efficient as O-demethylation on ring B, and this is probably why this compound was predicted to be more stable to metabolism than **8b**.

N-dealkylation of the nitrogen-containing side-chain was the principal route of metabolism for chloroquine and amodiaquine predicted by MetaSite. This result is in agreement with reported experimental findings, with their major metabolites identified as N-desethylchloroquine and N-desethylamodiaquine, respectively.[24;25] N-oxidation of the quinoline nitrogen, although highlighted by MetaSite as a possible site of metabolism, is not a favored route of metabolism for this class of compounds.

Unsurprisingly, N-dealkylation of the nitrogen-containing linkers was predicted as a possible route of metabolism for the proposed analogs. The piperazinyl-based linkers present in **22** – **27** were predicted as being particularly susceptible to N-dealkylation, possibly explaining why these compounds were predicted to be relatively unstable. This factor and the additional possibility of O-demethylation on ring B most likely explains why compound **23** was predicted to be the least stable of the analogs. The aminoethoxy linker present in **20** and **21** appears to be somewhat less susceptible to N-dealkylation, and was not predicted as the primary target of metabolism for these compounds, which were predicted to be the most stable of the studied analogs.

In summary, compounds **8b** and **12** showed poor predicted solubility profiles, suggesting limitations in oral bioavailability. They had acceptable predicted Caco2 permeation when compared to the reference compounds chloroquine and amodiaquine, though their metabolic stability was predicted to be lower. The proposed analogs had improved predicted solubilities relative to their parent compounds, particularly at lower pH, and this was a feature that could possibly be utilized during the solubilization of these analogs for *in vivo* pharmacokinetic (PK) studies. The analogs also maintained acceptably high predicted Caco2 permeability. On the basis of these predictions, the analogs were synthesized for *in vitro* antimalarial evaluation to determine if they retained antimalarial activity.

The main alert for the analogs was predicted metabolic instability, primarily due to N-dealkylation of the nitrogen-containing linkers or O-demethylation of ring B of the chalcone derivatives.

Synthesis

The hydroxylated enones (**15a** and **15b**) and chalcones (**16a** and **16b**) were intermediates in the synthesis of these compounds; the synthesis of these intermediates is depicted in Scheme 1, and involved the acid-catalyzed Claisen-Schmidt reaction.

Vanillin or 4-hydroxybenzaldehyde was stirred in acetone (as reagent and solvent) in the presence of aqueous 5M HCl at room temperature for 24 hours. The crude product of the reaction was purified by silica column chromatography to furnish the pure **15a** and **15b** in good yields. The synthesis of the chalcones **16a** and **16b** involved the reaction of vanillin or 4-hydroxybenzaldehyde with 1.1 equivalents of 2’,4’-dimethoxy-acetophenone in methanol, in the presence of aqueous HCl as catalyst. The crude products were then purified by silica gel column chromatography to furnish the pure chalcone intermediates in average yields.

Scheme 2 shows the synthesis of the target analogs **20** – **23**. The required hydroxylated quinoline intermediates **17** and **18** were afforded by typical aromatic substitution reactions using the (modified) method reported by Singh et al. 1971.[26] Briefly, 4,7-dichloroquinoline was heated with excess ethanolamine or with 1 equivalent of 1-(2-hydroxyethyl)piperazine in the presence of potassium carbonate to yield the target intermediates in moderate to good yield after purification by crystallization. The intermediates **17** and **18** were then coupled to either **15a** or **16a** to yield the target compounds **20** – **23**. This coupling was achieved by applying the Mitsunobu reaction, a convenient, one-step S_N2 reaction using 1.2 equivalents of triphenylphosphine (PPh_3) and 1.2 equivalents of diisopropyl azodicarboxylate (DIAD) as described by Winssinger et al. 2007.[27]

The synthesis of the proposed analogs **24** – **27** (Scheme 3) began with the synthesis of the piperazinyl intermediate **19** via an aromatic substitution reaction of 4,7-dichloroquinoline and 6 equivalents of piperazine, in the presence of potassium carbonate, using the (modified) method reported by Singh et al. 1971.[26] Purification by silica gel column chromatography afforded **19** in good yield. The Mannich reaction was then applied to furnish the target analogs using the (modified) method described by Chibale et al. 2007.[28] This involved the refluxing of the appropriate phenolic intermediate (**15** or **16**) and 1 equivalent of **19** in ethanol in the presence of 10 equivalents of aqueous formaldehyde for 12 hours. The crude products were then purified by silica gel column chromatography to afford the pure target compounds in average yields, which could be partly attributed to the fact that these reactions did not proceed to completion even with the use of a large excess of formaldehyde or after extended refluxing.

All compounds were characterized by ^{1}H-NMR, ^{13}C-NMR, Low Resolution Mass Spectrometry, IR Spectroscopy, Elemental analysis and melting point determination.

In vitro antiplasmodial assay results and discussion

The intermediates and target compounds were evaluated for their *in vitro* antiplasmodial activity against the chloroquine sensitive strain D10 and chloroquine resistant strains Dd2 and W2 of *P. falciparum* (Table 1).

The hydroxylated enone intermediate **15a** showed negligible antiplasmodial activity *in vitro* across all three strains of *P. falciparum*. However, the chalcone intermediate **16a** showed modest antiplasmodial activity against two of the three tested strains. The chloroquinoline-based intermediates **17** – **19** exhibited more potent antiplasmodial activity *in vitro*, with **19** showing sub-micromolar IC_{50} values against all three strains.

All the target analogs exhibited notable antiplasmodial activity, with IC_{50} values in the lower micromolar to mid-nanomolar range. The related analogs **25** and **27** were the most active of the analogs; both are chalcone derivatives with piperazinyl linkers, and had IC_{50} values between 0.3 – 0.6 μM against all three strains of *P. falciparum*. Compound **23** was also quite active, with mid-nanomolar IC_{50} values against the Dd2 and W2 *P. falciparum* strains.

Intermediate **19** was predicted by MetaSite as the main metabolite of **24** – **27** (arising from N-dealkylation of the linker), and the fact that it exhibited notable *in vitro* antiplasmodial potency implies that this intermediate/metabolite may contribute to *in vivo* antimalarial activity of these analogs, and thereby offset any potential liabilities of these compounds arising from susceptibility to metabolism *via* this route.

In summary, the replacement of the triazole linker in **8b** and **12** with the selected nitrogen-containing linkers was associated with retention of antiplasmodial activity, though none were as active as **8b**.

In vitro Metabolic Stability

The metabolic stability assay was performed by separately incubating test compounds at 37°C (in duplicate, substrate concentrations 1 μM) with human or mouse liver microsomes (0.4 mg/mL protein concentration). The reaction was initiated by the addition of an NADPH-regenerating system (containing 1 mg/mL NADP, 1 mg/mL glucose-6-phosphate, 1 U/mL glucose-6-phosphate dehydrogenase) and quenched at various time points over the incubation period by the addition of acetonitrile. . NADPH is the cofactor required for cytochrome P450-mediated metabolism. Additional samples with the dual cofactors NADPH and UDPGA (the latter the cofactor for glucuronidation) were included in the incubations for qualitative assessment of the potential for glucuronide formation. Control samples (containing neither NADPH nor UDPGA) were also included to monitor for potential degradation in the absence of cofactors. The concentrations of the substrates after the various periods of incubation were quantified against standard curves prepared in blank microsomal matrix by LC-MS using a Waters/Micromass ZQ mass spectrometer coupled to a Waters Alliance 2975 HPLC and an Ascentis Express C18 column maintained at a temperature of 40°C. Data processing was performed using Quanlynx software.

The results of the *in vitro* metabolism studies are summarized in Table 2. Two peaks were observed for **12, 22** and **23** during chromatographic LC-MS analysis, most likely indicating *cis* - *trans* isomerism occurring under assay conditions. The rates of degradation for each individual peak were therefore determined.

With respect to metabolic stability, the compounds exhibited varying degradation half-lives in human and mouse microsomes; however, the calculated hepatic extraction ratios (E_H values) were similar between the species. E_H values take into account the different hepatic blood flow rates between the species. The similarities in these values suggest no significant inter-species differences in the relative rates of metabolism.

Most of the compounds exhibited high E_H values (>0.7), suggesting notable susceptibility to hepatic metabolism. This is particularly apparent when compared to the relatively low values for chloroquine (≤0.31), and is in agreement with the prediction that this set of compounds would be less stable than chloroquine. Notably, **8b** and **27** had intermediate E_H values, as did the isomer of **23** corresponding to peak 2, indicating better metabolic stability than that of the other tested compounds.

The majority of the test compounds showed no measurable degradation in the microsomal matrix devoid of cofactors (i.e. controls), suggesting that there was no major non-cofactor dependent metabolism contributing to their rate of metabolism in liver microsomes. The only exceptions were **12** (peak 2) and **22** (peak 2), both of which demonstrated apparent non-cofactor dependent degradation (which was not observed for the other isomer), potentially indicating a stereo-specific process.

As noted above, the two peaks observed for **12, 22** and **23** during chromatographic LC-MS analysis suggested that there was possible *cis* - *trans* isomerism of these compounds under assay conditions. No obvious structural features specific to these compounds which would selectively predispose them to isomerism could be identified. The results suggest that one isomer of a compound could be more susceptible than the other to metabolism (e.g. compound **23**) or to additional routes of metabolism (e.g. peak 2 of compounds **12** and **22** to non-cofactor dependent hepatic metabolism). This non-uniform but notable influence of

isomerism on biological predisposition, and the fact that such isomerism may be random and unpredictable even among closely related compounds, underscored the need for close attention when studying compounds containing systems potentially capable of isomerization, such as the α-β unsaturated system present in enones and chalcones.

Putative Metabolite Identification

The MS scan data from the metabolic stability assay of each compound was screened for the presence of fragments corresponding to putative metabolites; data acquisition was conducted in MS scan mode (spectra acquired from 100 to 1000 Daltons). It should be noted that, in the absence of authentic metabolites, the chromatographic conditions in each case were optimized for each parent compound and the identities of the putative metabolites were not confirmed by dedicated MS-MS experiments.

With respect to routes/sites of metabolism, the metabolite profiles of all the examined compounds were found to be similar across the two species tested. Oxygenation (P+16, P +32), O-demethylation (P−14) and N-dealkylation (P−174, P−218, P−240, P−296, P−326, P−326) appeared to be the predominant pathways, where P is the molecular mass of the parent compound.

This was consistent with the site-of-metabolism predictions derived from MetaSite (Figure 4), where these three were the major predicted routes of metabolism. However, there were differences between the predicted routes of metabolism and detected metabolites for some of the compounds; for example, no predicted O-demethylation metabolites were detected for **8b** and **20**, and no N-dealkylation metabolite was detected for **21**.

For compounds with the piperazine linkers (**22** – **27**) a common metabolite with *m/z* of 248 Daltons was found (i.e. P – 218 [**22**]; P – 340 [**23**]; P – 204 [**24**]; P – 326 [**25**]; P – 174 [**26**]; and P – 296 [**27**]). This was consistent with N-dealkylation of the side chain from the piperazine, and was confirmation of this route of metabolism as predicted by MetaSite for all the piperazinyl-based analogs. For **20**, N-dealkylation of the amino-ethoxy linker was observed, resulting in the generation of a metabolite with *m/z* 179 Daltons (i.e. P – 218); this was not observed for **21**, which also bears an amino-ethoxy linker. The putative metabolites from these N-dealkylation reactions are shown in Figure 5.

The potential of the test compounds to undergo primary glucuronidation was assessed in the microsomal incubation by the addition of the cofactor UDPGA. There was no major increase in the rate of degradation of **8b, 20, 21, 23**, or chloroquine in microsomal samples containing NADPH and UDPGA relative to those containing NADPH alone, suggesting that these compounds were not susceptible to primary glucuronidation. For **12** and **22**, the impact of UDPGA on the overall rate of metabolism could not be assessed, as the rate of NADPH-dependent degradation alone was too rapid. However, for these two compounds, there were no putative metabolites detected with molecular weights consistent with glucuronidation.

In contrast to the results discussed above, there was evidence of primary glucuronidation for **24** – **27** in the microsomal assay, where there was an increase in the relative rates of degradation of test compounds in the presence of UDPGA and/or the detection of a putative metabolite with a molecular weight consistent with glucuronide conjugation [P + 176]. Each of these compounds bear a free phenolic –OH group, and it is therefore not surprising that they are substrates for glucuronidation. This route of metabolism was not predicted by MetaSite, which only predicts cytochrome P450-mediated phase I metabolism.

Physicochemical properties – solubility and partition coefficients

The partition coefficients (logD) of the test compounds were estimated using a modification of the method described by Lombardo and co-workers[29] (Table 3). The series exhibited moderate to high partition coefficients, with measured $logD_{7.4}$ values ranging from 3.0 to 5.3. Under acidic conditions (pH 3.0), the majority of compounds showed a reduction in logD values, consistent with ionization of the weakly basic groups; however, the logD values of the neutral **8b** and **12** were unchanged across the pH range tested. The above predictions were consistent with the *in silico* predicted results. Compounds **24** and **26** had notably lowed $logD_{3.0}$ values, reflecting the dual ionization of the piperazinyl and quinoline nitrogens under acidic conditions, as well as their lower molecular weights (relative to **25** and **27**, respectively). The partition coefficients for chloroquine were lower than those observed for the novel compounds.

The solubility of the test compounds was estimated using the turbidimetric method described by Bevan and Lloyd,[30] applying standard test buffers (pH 2.0 and 6.5). As predicted, the solubility characteristics of the series were relatively poor at pH 6.5, with only **20** showing moderate solubility under neutral conditions (Table 3). Under acidic conditions, compounds **20** –**27** showed improved solubility consistent with ionization of the basic centres within the structures. **8b** and **12** showed no increase in solubility under acidic conditions, consistent with the neutral characteristics of these triazole substituted compounds. Chloroquine showed good solubility under both neutral and acidic conditions.

Mechanistic studies

A limited investigation was carried out on the synthesized analogs in an attempt to elucidate their mechanisms of action. The mechanisms considered for investigation were based on literature accounts of the possible mechanisms by which chalcones and quinoline-containing compounds exert their antimalarial activities.

Inhibition of hemozoin formation is an attractive target for antimalarial drugs, and quinoline-based antimalarials such as chloroquine and amodiaquine are proposed to exert their antimalarial activity via this mechanism.[17;31;32] The plasmodial cysteine proteases involved in hemoglobin catabolism, such as falcipain 2, have also been proposed as potential antimalarial targets.[33;34] By possessing α-β unsaturated carbonyl groups and thereby able to act as Michael acceptors, chalcones could potentially irreversibly inhibit the thiol-containing malarial cysteine proteases;[18] several quinolinyl chalcones which are moderate inhibitors of falcipain 2 have been identified.[35] Some chalcones have also been shown to inhibit new permeability pathways (NPPs), which are parasite-induced solute channels in erythrocyte membranes.[36] Considering these potential targets, a selection of intermediates and analogs were evaluated for inhibition of β-hematin formation, falcipain 2 activity, and NPP function (sorbitol-induced hemolysis of infected erythrocytes) (Table 4).

Compound **8b**, the most potent compound *in vitro*, was only slightly more potent (IC_{50} 1.6 equiv.) than chloroquine in inhibiting β-hematin formation. Of the analogs tested, compounds **20** – **27** were all very potent (more potent than chloroquine) inhibitors of β-hematin formation. Compounds **23** and **27** (which were also some of the more active of these analogs) had the lowest values of 0.2 equiv. Thus, inhibition of hemozoin formation may be a primary mechanism of antimalarial action of these compounds. The intermediates **17** – **19** showed only moderate inhibition of β-hematin formation. Interestingly, the hydroxylated chalcone **16b**, which showed activity comparable to that of chloroquine, while the chalcone and enone intermediates **15a, 15b** and **16a** showed negligible β-hematin inhibition activity.

The analogs showed moderate to poor inhibition of falcipain 2 relative to E64, a known, potent inhibitor of the enzyme; only compound **8b** and the analogs **21, 23, 25, 26** and **27** had lower micromolar IC_{50} values. The chalcone/enone intermediates **15** – **16** and the quinoline intermediates **17** – **19** did not show appreciable falcipain 2 inhibition even at a concentration of 50 μM. The relatively low potencies of compounds **20, 22** and **24** as falcipain 2 inhibitors suggested that this was not the primary mechanism of antimalarial action of these compounds. However, the most potent analogs against falcipain 2, **23, 25**, and **27**, were among the most potent against cultured parasites, suggesting that protease inhibition may play a role in the mechanism of action of these compounds.

All analogs tested were poor inhibitors of sorbitol-induced lysis, with **24**, the most active compound, with only 17% inhibition. This result discounts inhibition of NPPs as a mechanism of action for these analogs.

Summary and conclusions

8b and **12** were selected for structural modification, with the aim of identifying analogs with improved solubility and which retained antimalarial potency. Eight analogs were proposed, and these were characterized *in silico* for selected physicochemical and ADME parameters. These analogs were predicted to have improved solubilities relative to the parent compounds, particularly at low pH; they retained acceptable predicted Caco2 permeability, but were identified as possible substrates for metabolism, principally N-dealkylation by hepatic cytochromes.

The proposed analogs were then synthesized and tested, and were found to exhibit notable *in vitro* antiplasmodial activity, though none were as active as **8b**. Compounds **25** and **27** were the most active of the analogs. **19**, an intermediate in the synthesis (and a putative metabolite) of some of the analogs was also found to exhibit notable antiplasmodial activity.

There was no evidence of significant inter-species differences in the relative rates of microsomal metabolism of these compounds between mice and humans. However, most of the compounds exhibited high E_H values (>0.7), suggesting considerable susceptibility to hepatic metabolism. Oxygenation, O-demethylation and N-dealkylation appeared to be the predominant metabolic pathways, which was consistent with the site-of-metabolism predictions derived from MetaSite. There was also evidence of primary glucuronidation for **24** – **27**. The majority of the compounds showed no susceptibility to metabolism by enzymes other than hepatic cytochromes and transferases.

Inhibition of hemozoin formation was found to be a likely mechanism by which the tested analogs exert their antiplasmodial activity. Analogs **20** – **27** were all more potent than chloroquine in inhibiting β-hematin formation. Inhibition of falcipain 2 could also contribute to the observed antiplasmodial activities of some of these compounds, while inhibition of parasite-induced transport channels did not appear to be a notable mechanism of action.

The proposed analogs were by no means exhaustive, but represented compounds that did not represent significant deviations from the molecules known to be active, and were therefore more likely to retain activity. They consisted of a small range of compounds that that could be conveniently synthesized, and which offered possible improvements on certain physicochemical and/or ADME properties of the parent compounds, particularly solubility. In addition, they opened up possibilities for further derivatization in future.

The more promising compounds **25** and **27** were evaluated for their cytotoxicity against the Chinese Hamster Ovarian (mammalian) cell line. No cytotoxicity was observed at the

highest concentration (100 μM) tested, an observation that was consistent with the findings previously reported for compound **8b**.[16]

Experimental

To guide in the interpretation of the ^{1}H-NMR data presented below, the complete (and numbered) structures of all the intermediates and target compounds can be found in the Supporting Information. This material is available free of charge via the Internet at http://pubs.acs.org. Purity was determined by combustion analysis, and all compounds were confirmed to have > 95% purity.

7.1 General Method A for the preparation of compounds 15a and 15b

Vanillin or 4-hydroxybenzaldehyde (20 mmol) was dissolved in 30 mL acetone, and 5 mL of 5 M HCl was then added gradually to the stirring mixture. The reaction mixture was then stirred at room temperature for 24 hours. The reaction mixture was then neutralized with 2.5 M NaOH, after which the acetone in the mixture was removed at reduced pressure. The remaining compound mixture was then taken up in 100 mL EtOAc, washed three times with water, dried over anhydrous Na_2SO_4, concentrated *in vacuo* and purified by column chromatography (EtOAc/Hexane) to yield the pure target compound.

7.1.1 4-(4-Hydroxy-3-methoxy-phenyl)-but-3-en-2-one 15a—Pale yellow solid (3.2 g, 84%); mp 124 – 125°C (from EtOAc/Hex); R_f (EtOAc:Hex 4:6) 0.30; IR ν_{max} (KBr)/ cm^{-1} 3261 (Ar O-H), 3000 (Ar C-H), 1668 (C=O), 1581 (Ar C=C); δ_H (400 MHz, $CDCl_3$) 7.46 (1H, d, *J* 16.2, H-a), 7.09 (1H, dd, *J* 1.9 and 8.2, H-2), 7.07 (1H, d, *J* 1.9, H-1), 6.94(1H, d, *J* 8.1, H-3), 6.60 (1H, d, *J* 16.2, H-b), 5.98 (1H, s, H-5), 3.95 (3H, s, H-4), 2.37 (3H, s, H-b'); δ_C (100 MHz, $CDCl_3$) 198.3, 150.4, 146.9, 143.5, 126.5, 125.0, 123.8, 114.9, 109.4, 55.8, 24.5; LRMS (EI) m/z 193.1 (MH^+); Anal. ($C_{11}H_{12}O_3$) C H.

7.1.2 4-(4-Hydroxy-phenyl)-but-3-en-2-one 15b—Dark yellow solid (2.4 g, 76%); mp 81 – 82°C (from EtOAc/Hex); R_f (EtOAc:Hex 4:6) 0.40; IR ν_{max} (KBr)/cm^{-1} 3150 (Ar C-H), 1666 (C=O), 1590 (Ar C=C); δ_H (400 MHz, $CDCl_3$) 7.50 (1H, d, *J* 16.2, H-a), 7.42 (2H, d, *J* 8.7, H-1, 2), 6.88 (2H, d, *J* 8.7, H-3, 4), 6.58 (1H, d, *J* 16.2, H-b), 2.35 (3H, s, H-b'); δ_C (100 MHz, $CDCl_3$) 200.0, 159.1, 144.8, 130.4 (2C), 126.5, 124.3 (2C), 116.2, 27.2; LRMS (EI) m/z 163.3 (MH^+); Anal. ($C_{10}H_{10}O_2$) C H.

7.2 General Method B for the preparation of compounds 16a and 16b

Vanillin or 4-hydroxybenzaldehyde (20 mmol) and 2,4-dimethoxyacetophenone (4.0 g, 22 mmol) were dissolved in 20 mL MeOH. 5 mL of 5 M HCl was then added gradually to the stirring mixture. The reaction mixture was then stirred at 50°C for 24 hours. The reaction mixture was then allowed to cool to ambient temperature and neutralized with 2.5 M NaOH, after which the MeOH in the mixture was removed under reduced pressure. The remaining compound mixture was then taken up in 100 mL EtOAc, washed three times with water, dried over anhydrous Na_2SO_4, concentrated *in vacuo* and purified by column chromatography (EtOAc/Hexane) to yield the pure target compound.

7.2.1 1-(2,4-Dimethoxy-phenyl)-3-(4-hydroxy-3-methoxy-phenyl)-propenone 16a—Yellow solid (4.3 g, 68%); mp 92 – 94°C (from EtOAc /Hex); R_f (EtOAc:Hex 4:6) 0.30; IR ν_{max} (KBr)/cm^{-1} 3506 (Ar O-H), 3113 (Ar C-H), 1640 (C=O), 1598 (Ar C=C); δ_H (400 MHz, $CDCl_3$) 7.74 (1H, d, *J* 8.6, H-3'), 7.61 (1H, d, *J* 15.7, H-a), 7.35 (1H, d, *J* 15.7, H-b), 7.17 (1H, dd, *J* 1.9 and 8.3, H-2), 7.10 (1H, d, *J* 1.9, H-1), 6.94 (1H, d, *J* 8.3, H-3), 6.58 (1H, dd, *J* 2.3 and 8.6, H-2'), 6.51 (1H, d, *J* 2.3, H-1'), 5.93 (1H, s, H-5), 3.94 (3H, s, H-4'), 3.91 (3H, s, H-5'), 3.88 (3H, s, H-4); δ_C (100 MHz, $CDCl_3$) 190.8, 163.9, 160.2,

147.8, 146.7, 142.6, 132.6, 128.0, 125.1, 122.8, 122.5, 114.8, 110.2, 105.1, 98.8, 55.9, 55.8, 55.5; LRMS (EI) m/z 314.0 (M^+); Anal. ($C_{18}H_{18}O_5$.) C H.

7.2.2 1-(2,4-Dimethoxy-phenyl)-3-(4-hydroxy-3-methoxy-phenyl)-propenone 16b—Yellow solid (3.2 g, 59%); mp 92 – 94°C (from EtOAc /Hex); R_f (EtOAc:Hex 4:6) 0.27; IR ν_{max} (KBr)/cm^{-1} 3204 (Ar O-H), 1635 (C=O), 1600(Ar C=C); δ_H (400 MHz, $CDCl_3$) 7.53 (2H, d, *J* 8.7, H-1, 2), 7.51 (1H, d, *J* 8.7, H-3'), 7.43 (1H, d, *J* 15.8, H-a), 7.28 (1H, d, *J* 15.7, H-b), 6.78 (2H, d, *J* 8.5, H-3, 4), 6.62 (1H, d, *J* 2.1, H-1'), 6.58 (1H, dd, *J* 2.0 and 8.6, H-2'), 3.83 (3H, s, H-4'), 3.79 (3H, s, H-5'); δ_C (100 MHz, $CDCl_3$) 189.9, 164.1, 160.4, 160.3, 142.4, 132.3, 130.8, 126.3, 124.3, 122.3, 116.4, 106.4, 99.2, 56.4, 56.0; LRMS (EI) m/z 284.0 (M_+); Anal. ($C_{17}H_{16}O_4$)- C H.

7.3 2-(7-Chloro-quinolin-4-ylamino)-ethanol 17

4,7-dichloroquinoline (2 g, 10mmol) was heated with stirring in neat ethanolamine (10 mL) at 130 °C for 5 hours. The mixture was then allowed to cool to room temperature, during which the compound **17** precipitated. This crude mixture was then suspended in water, filtered and crystallized from hot MeOH to yield pure **17** as a white solid (1.97 g, 89%). Mp 215 – 216°C (from MeOH) (lit. 214 °C)[37] R*f* (MeOH/EtOAc, 1:9) 0.20; δ_H (400 MHz; DMSO-d_6) 8.41 (1H, d, *J* 5.4, H2), 8.30 (1H, d, *J* 9.0, H5), 7.81 (1H, d, *J* 2.2, H3), 7.46 (1H, dd, *J* 2.2 and 8.9, H4), 7.26 (1H, t, *J* 5.2, H-6), 6.52 (1H, d, *J* 5.5, H1), 4.85 (1H, s, H-9), 3.70 (2H, t, *J* 5.9, H8), 3.38 (2H, q, *J* 5.8, H7).

7.4 2-[4-(7-Chloro-quinolin-4-yl)-piperazin-1-yl]-ethanol 18

4,7-dichloroquinoline (2 g, 10mmol) was dissolved in 10 mL anhydrous DMF, after which K_2CO_3 (2.1 g, 15 mmol) and 1-(2-hydroxyethyl)piperazine (1.3 g, 10 mmol) were added. This reaction mixture was then stirred at 80 °C for 24 hrs, upon which TLC indicated completion of the reaction. The mixture was then diluted in 100 mL EtOAc, washed with water (2 × 30 mL), dried over anhydrous Na_2SO_4 and concentrated under reduced pressure. The resultant oily product crystallized on standing, and these crystals were washed with hexane and dried to yield **18** as pale yellow crystals (1.83 g, 63%). M.p. 111 – 112°C (from EtOAc); R_f (MeOH/EtOAc, 1:9) 0.24; IR ν_{max} ($CHCl_3$)/cm^{-1} 3222 (O-H), 2903 (C-H), 1677 (C=O), 1569 (Ar C=C); δ_H (400 MHz, DMSO-d_6) 8.66 (1H, d, *J* 5.0, H-2), 7.99 (1H, d, *J* 9.0, H-5), 7.95 (1H, d, *J* 2.2, H-3), 7.51 (1H, dd, *J* 2.2 and 9.0, H-4), 6.96 (1H, d, *J* 5.1, H-1), 4.33 (1H, t, *J* 5.3, H-12), 3.55 (2H, q, *J* 6.0, H-11), 3.17 (4H, t, *J* 4.8, H-6, 9), 2.70 (4H, t, *J* 4.8, H-7, 8), 2.51 (2H, t, *J* 6.2, H-10); δ_C (100 MHz, $CDCl_3$) 156.2, 151.9, 149.6, 133.4, 127.9, 125.9, 125.5, 121.3, 109.1, 60.0, 58.5 (2C), 52.8 (2C), 51.7; LRMS (EI) m/z 290.5 (M^+); Anal. ($C_{15}H_{18}ClN_3O$) C H N.

7.5 7-Chloro-4-piperazin-1-yl-quinoline 19

4,7-dichloroquinoline (2 g, 10mmol) was dissolved in 15 mL anhydrous NMP, after which K_2CO_3 (2.8 g, 20 mmol) and piperazine (5.2 g, 60 mmol) were added. This reaction mixture was then stirred at 135 °C for 4 hrs, upon which TLC indicated completion of the reaction. The mixture was then diluted in 100 mL EtOAc, washed with water (2 × 30 mL), dried over anhydrous Na_2SO_4, concentrated under reduced pressure and purified by column chromatography (NH_4OH/MeOH/EtOAC, 1:9:90) to yield **19** as an off-white solid (1.9 g, 78%). M.p. 111 – 112°C (lit. 113 – 115 °C)[26]; δ_H (400 MHz, DMSO-d_6) 8.68 (1H, d, *J* 5.0, H-2), 8.01 (1H, d, *J* 9.0, H-3), 7.89 (1H, d, *J* 2.0, H-5), 7.52 (1H, dd, *J* 2.1 and 9.0, H-4), 6.95 (1H, d, *J* 5.0, H-1), 3.05 – 3.11 (4H, m, H-6, 9), 2.92 – 2.97 (4H, m, H-7, 8), 3.19 (1H, br s, H-10); δ_C (100 MHz, DMSO-d_6) 157.4, 152.6, 150.2, 133.9, 128.5, 126.6, 121.9, 109.7, 53.7 (2C), 45.9 (2C).

7.6 General Method C for the preparation of compounds 20 – 23

Hydroxylated chloroquinoline intermediate **17** or **18** (1 eq.), enone **15a** or chalcone **16a** (1 eq.) and triphenylphosphine (1.2 eq.) were dissolved in anhydrous DCM under a N_2 atmosphere. The solution was cooled to 0°C, and di-isopropyl azodicarboxylate (DIAD, 1.2 eq.) was added slowly over 5 min. The stirred reaction mixture was then allowed to warm to ambient temperature, and was further stirred for 6 hrs. The mixture was then concentrated under reduced pressure, and the target compound purified by silica column chromatography (5% MeOH in EtOAc).

7.6.1 4-{4-[2-(7-Chloro-quinolin-4-ylamino)-ethoxy]-3-methoxy-phenyl}-but-3-en-2-one 20—Yellow solid (289 mg, 73%); mp 143 – 144°C (from MeOH/EtOAc); R_f (MeOH/EtOAc 1:9) 0.23; IR ν_{max} (KBr)/cm^{-1} 3420 (N-H), 2972 (Ar C-H), 1686 (C=O), 1584 (Ar C=C); δ_H (400 MHz, $CDCl_3$) 8.57 (1H, d, *J* 5.3, H-9), 7.99 (1H, d, *J* 1.8, H-10), 7.76 (1H, d, *J* 8.9, H-12), 7.46 (1H, d, *J* 16.2, H-a), 7.39 (1H, dd, *J* 1.9 and 8.9, H-11), 7.13-7.11 (2H, m, H-1, 2), 6.98 (1H, d, *J* 8.0, H-3), 6.63 (1H, d, *J* 16.2, H-b), 6.49 (1H, d, *J* 5.3, H-8), 5.70 (1H, s, H-7), 4.39 (2H, t, H-5.0, H-5), 3.92 (3H, s, H-4), 3.73 (2H, q, *J* 5.0, H-6), 2.37 (3H, s, H-a'); δ_C (100 MHZ, $CDCl_3$) 198.2, 151.7, 150.1, 149.8, 148.9, 142.9, 135.1, 128.9, 125.9, 125.5, 122.6, 121.2, 117.4, 114.7, 110.5, 99.3, 67.7, 55.8, 42.3, 27.4, 21.9; LRMS (EI) m/z 395.3 $(M - H)^+$; Anal. ($C_{22}H_{21}ClN_2O_3$) C H N.

7.6.2 3-{4-[2-(7-Chloro-quinolin-4-ylamino)-ethoxy]-3-methoxy-phenyl}-1-(2,4-dimethoxy-phenyl)-propenone 21—Pale yellow solid (310 mg, 60%); mp 164 – 166°C (from MeOH/EtOAc); R_f (MeOH:EtOAc 1:9) 0.27; IR ν_{max} (KBr)/cm^{-1} 3406 (N-H), 2942 (Ar C-H), 1646 (C=O), 1584 (Ar C=C); δ_H (400 MHz, $CDCl_3$) 8.57 (1H, d, *J* 5.3, H-9), 7.98 (1H, d, *J* 2.1, H-10), 7.78-7.74 (2H, m, H-3', 12), 7.61 (1H, d, *J* 15.7, H-a), 7.39 (1H, d, *J* 15.7, H-b), 7.38 (1H, dd, *J* 2.1 and 8.9, H-11), 7.17 (1H, dd, *J* 1.7 and 8.2, H-2), 7.14 (1H, d, *J* 1.7, H-1), 6.96 (1H, d, *J* 8.2, H-3), 6.57 (1H, dd, 2.2 and 8.6, H-2'), 6.52 (1H, d, *J* 2.2, H-1'), 6.48 (1H, d, *J* 5.3, H-8), 5.78 (1H, t, *J* 5.5, H-7), 4.39 (2H, t, *J* 5.2, H-5), 3.92 (3H, s, H-4'), 3.90 (3H, s, H-5'), 3.88 (3H, s, H-4), 3.72 (2H, q, *J* 5.2, H-6); δ_C (100 MHZ, $CDCl_3$) 190.5, 164.1, 160.3, 152.0, 150.1, 149.6, 149.4, 149.2, 141.8, 134.9, 132.7, 130.2, 128.9, 126.1, 125.4, 122.3, 122.2, 121.2, 117.5, 115.0, 111.2, 105.2, 99.3, 98.8, 67.8, 55.9, 55.7, 55.5, 42.3; LRMS (EI) m/z 517.1 $(M - H)^+$; Anal. ($C_{29}H_{27}ClN_2O_5$) C H N.

7.6.3 4-(4-{2-[4-(7-Chloro-quinolin-4-yl)-piperazin-1-yl]-ethoxy}-3-methoxy-phenyl)-but-3-en-2-one 22—Pale yellow (316 mg, 68%); mp 61 – 62°C (from MeOH/EtOAc); R_f (MeOH/EtOAc 1:9) 0.26; IR ν_{max} (KBr)/cm^- 2977 (Ar C-H), 1714 (C=O), 1594 (Ar C=C); δ_H (300 MHz, $CDCl_3$) 8.72 (1H, d, *J* 5.0, H-12), 8.04 (1H, d, *J* 2.0, H-13), 7.93 (1H, d, *J* 8.9, H-15), 7.46 (1H, d, *J* 16.1, H-a), 7.41 (1H, dd, *J* 2.2 and 9.0, H-14), 7.12 (1H, dd, *J* 1.9 and 8.3, H-2), 7.09 (1H, d, *J* 1.9, H-1), 6.92 (1H, d, *J* 8.2, H-3), 6.83 (1H, d, *J* 5.0, H-11), 6.61 (1H, d, *J* 16.1, H-b), 4.25 (2H, t, *J* 5.9, H-5), 3.90 (3H, s, H-4), 3.28-3.25 (4H, m, H-8, 9), 2.99 (2H, t, *J* 5.9, H-6), 2.91-2.88 (4H, m, H-7, 10), 2.36 (3H, s, H-a'); δ_C (75 MHZ, $CDCl_3$) 198.0, 156.9, 151.9, 150.5, 150.1, 149.7, 143.2, 134.8, 128.8, 127.8, 126.1, 125.4, 125.1, 122.7, 113.0, 110.3, 108.9, 67.0, 56.8, 55.9, 53.4, 52.9, 52.1, 27.3, 21.9; LRMS (EI) m/z 464.2 $(M - H)^+$; Anal. ($C_{26}H_{28}ClN_3O_3$) C H N.

7.6.4 3-(4-{2-[4-(7-Chloro-quinolin-4-yl)-piperazin-1-yl]-ethoxy}-3-methoxy-phenyl)-1-(2,4-dimethoxy-phenyl)-propenone 23—Yellow solid (435 mg, 74%); mp 62 – 63°C (from MeOH/EtOAc); R_f (MeOH/EtOAc 1:9) 0.30; IR ν_{max} (KBr)/cm^{-1} 2938 (C-H), 1648 (C=O), 1600 (Ar C=C); δ_H (300 MHz, $CDCl_3$) 8.66 (1H, d, *J* 5.0, H-12), 8.01 (1H, d, *J* 9.0, H-15), 7.95 (1H, d, *J* 2.1, H-13), 7.56 (1H, d, *J* 8.5, H-3'), 7.53 (1H, dd, *J* 2.3 and 9.0, H-14), 7.46 (1H, d, *J* 15.8, H-a), 7.37 (1H, d, *J* 15.8, H-b), 7.30 (1H, d, *J* 1.9, H-1), 7.23 (1H, dd, *J* 1.9 and 8.4, H-2), 7.05 (1H, d, *J* 8.4, H-3), 6.99 (1H, d, *J* 5.1, H-11), 6.67

(1H, d, *J* 2.2, H-1'), 6.62 (1H, dd, *J* 2.2 and 8.6, H-2'), 4.19 (2H, t, *J* 5.8 H-5), 3.87 (3H, s, H-4'), 3.84 (3H, s, H-5'), 3.83 (3H, s, H-4), 3.19 (4H, t, *J* 4.8, H-8, 9), 2.85 (2H, t, *J* 5.8, H-6), 2.79 (4H, t, *J* 4.8, H-7, 10); δ_C (75 MHZ, $CDCl_3$) 189.7, 163.5, 159.9, 156.2, 151.9, 150.1, 149.6, 149.2, 141.6, 133.4, 131.5, 127.9, 125.8, 125.5, 125.1, 122.3, 121.7, 121.2, 113.3, 111.4, 109.2, 105.8, 98.7, 65.6, 56.3, 55.8 (2C), 52.8 (2C), 51.7 (2C); LRMS (EI) m/z 586.0 $(M - H)^+$; Anal. ($C_{33}H_{34}ClN_3O_5$) C H N.

7.7 General Method D for the preparation of compounds 24 – 27

The appropriate hydroxylated chalcone or enone (**15** or **16**) (1 eq.) and the piperazinylquinoline intermediate, **19** (1 eq) were dissolved in EtOH. Formaldehyde (37% solution in water, 10 eq.) was then added to the stirring solution, which was then refluxed at 110°C for 12 hrs. The reaction mixture was then allowed to cool to ambient temperature, after which it was concentrated under reduced pressure and purified by column chromatography (EtOAc) to yield the pure target compounds.

7.7.1 4-{3-[4-(7-Chloro-quinolin-4-yl)-piperazin-1-ylmethyl]-4-hydroxy-5-methoxyphenyl}-but-3-en-2-one 24—Yellow solid (58%); mp 91 – 92°C (from EtOAc); R_f (EtOAc) 0.15; IR ν_{max} (KBr)/cm^{-1} 2943 (C-H), 1662 (C=O), 1575 (Ar C=C); δ_H (300 MHz, $CDCl_3$) 8.73 (1H, d, *J* 5.0, H-11), 8.06 (1H, d, *J* 2.1, H-12), 7.89 (1H, d, *J* 9.0, H-14), 7.43 (1H, d, *J* 16.1, H-a), 7.40 (1H, dd, *J* 2.1 and 9.0, H-13), 7.03 (1H, d, *J* 1.5, H-2), 6.91 (1H, d, *J* 1.5, H-1), 6.82 (1H, d, *J* 5.0, H-10), 6.58 (1H, d, *J* 16.1, H-b), 3.91 (3H, s, H-3), 3.89 (2H, s, H-5), 3.28 – 3.34 (4H, m, H-7, 8), 2.90 – 2.96 (4H, m, H-6, 9), 2.35 (3H, s, H-a'); δ_C (75 MHz, $CDCl_3$) 198.1, 156.4, 151.6, 149.9, 149.6, 148.4, 143.5, 135.2, 128.8, 126.5, 125.8, 124.9, 124.8, 122.5, 121.7, 120.9, 110.1, 109.1, 60.7, 55.9, 52.4 (2C), 51.9 (2C), 27.4; LRMS (EI) m/z 450.7 $(M - H)^+$; Anal. ($C_{25}H_{26}ClN_3O_3.H_2O$) C H N.

7.7.2 3-{3-[4-(7-Chloro-quinolin-4-yl)-piperazin-1-ylmethyl]-4-hydroxy-5-methoxyphenyl}-1-(2,4-dimethoxy-phenyl)-propenone 25—Deep yellow solid (66%); mp 95 – 97°C (from EtOAc); R_f (EtOAc) 0.20; IR ν_{max} (KBr)/cm^{-1} 2938 (C-H), 1648 (C=O), 1597 (Ar C=C); δ_H (400 MHz, $CDCl_3$) 8.71 (1H, d, *J* 5.1, H-11), 8.10 (1H, d, *J* 1.9, H-12), 7.89 (1H, d, *J* 9.0, H-14), 7.72 (1H, d, *J* 8.6, H-3'), 7.58 (1H, d, *J* 15.8, H-a), 7.44 (1H, dd, *J* 1.9 and 8.9, H-13), 7.33 (1H, d, *J* 15.7, H-b), 7.09 (1H, d, *J* 1.8, H-2), 6.97 (1H, d, *J* 1.8, H-1), 6.84 (1H, d, *J* 5.1, H-10), 6.57 (1H, dd, *J* 1.7 and 8.6, H-2'), 6.51 (1H, d, *J* 1.8, H-1'), 3.92 (3H, s, H-4'), 3.91 (5H, s, H-5, 5'), 3.87 (3H, s, H-3), 3.32 – 3.55 (4H, m, H-7, 8), 2.90 – 2.96 (4H, m, H-6, 9); δ_C (100 MHz, $CDCl_3$) 190.9, 163.9, 160.3, 156.7, 151.2, 149.4, 149.2, 148.3, 142.5, 135.5, 132.6, 128.4, 126.6, 124.9, 124.8, 122.7, 122.6, 121.6, 120.7, 110.8, 110.5, 109.0, 105.2, 98.8, 60.6, 56.0, 55.8, 55.5, 52.3 (2C), 51.8 (2C); LRMS (EI) m/z 572.7 $(M - H)^+$; Anal. ($C_{32}H_{32}ClN_3O_5.H_2O$) C H N.

7.7.3 4-{3-[4-(7-Chloro-quinolin-4-yl)-piperazin-1-ylmethyl]-4-hydroxy-phenyl}-but-3-en-2-one 26—Pale yellow solid (45%); mp 83 – 85°C (from EtOAc); R_f (EtOAc) 0.35; IR ν_{max} (KBr)/cm^{-1} 2823 (C-H), 1663 (C=O), 1578 (Ar C=C); δ_H (300 MHz, $CDCl_3$) 8.71 (1H, d, *J* 5.1, H-11), 8.07 (1H, d, *J* 2.1, H-12), 7.89 (1H, d, *J* 9.0, H-14), 7.44 (1H, d, *J* 16.4, H-a), 7.43 (1H, dd, *J* 2.1 and 9.0, H-13), 7.41 (1H, dd, *J* 2.3 and 8.4, H-2), 7.30 (1H, d, *J* 2.3, H-1), 6.86 (1H, d, *J* 8.4, H-3), 6.85 (1H, d, *J* 5.1, H-10), 6.58 (1H, d, *J* 16.3, H-b), 3.88 (2H, s, H-5), 3.28 – 3.35 (4H, m, H-7, 8), 2.85 – 2.93 (4H, m, H-6, 9), 2.34 (3H, s, H-a'); δ_C (75 MHz, $CDCl_3$) 198.2, 160.1, 156.5, 151.5, 149.7, 143.2, 135.3, 129.8, 129.1, 128.7, 126.5, 126.0, 124.8, 124.6, 121.7, 121.1, 116.9, 109.1, 61.2, 52.4 (2C), 51.9 (2C), 27.4; LRMS (EI) m/z 420.7 $(M - H)^+$; Anal. ($C_{24}H_{24}ClN_3O_2.H_2O$) C H N.

7.7.4 3-{3-[4-(7-Chloro-quinolin-4-yl)-piperazin-1-ylmethyl]-4-hydroxy-phenyl}-1-(2,4-dimethoxy-phenyl)-propenone 27—Yellow solid (49%); mp 85 –

87°C (from EtOAc); R_f (EtOAc) 0.40; IR ν_{max} (KBr)/cm^{-1} 2935 (C-H), 1649 (C=O), 1598 (Ar C=C); δ_H (400 MHz, $CDCl_3$) 8.68 (1H, d, *J* 5.0, H-11), 8.07 (1H, d, *J* 1.8, H-12), 7.89 (1H, d, *J* 9.0, H-14), 7.69 (1H, d, *J* 8.6, H-3'), 7.57 (1H, d, *J* 15.7, H-a), 7.46 (1H, dd, *J* 1.9 and 8.5, H-2), 7.41 (1H, dd, *J* 1.8 and 8.9, H-13), 7.32 (1H, d, *J* 15.7, H-b), 7.24 (1H, d, *J* 1.9, H-1), 6.83 (1H, d, *J* 8.3, H-3), 6.82 (1H, d, *J* 4.9, H-10), 6.52 (1H, dd, *J* 2.0 and 8.6, H-2'), 6.47 (1H, d, *J* 2.0, H-1'), 3.87 (3H, s, H-4'), 3.85 (2H, s, H-5), 3.83 (3H, s, H-5'), 3.28 – 3.34 (4H, m, H-7, 8), 2.84 – 2.90 (4H, m, H-6, 9); δ_C (100 MHz, $CDCl_3$) 190.6, 163.9, 160.2, 159.6, 156.7, 151.1, 149.3, 142.1, 135.5, 132.6, 129.6, 129.3, 128.4, 127.1, 126.6, 124.8, 124.6, 122.5, 121.5, 120.8, 116.9, 108.9, 105.1, 98.7, 61.55, 55.7, 55.4, 52.4 (2C), 51.8 (2C); LRMS (EI) m/z 542.8 (M^+); Anal. ($C_{31}H_{30}ClN_3O_4.H_2O$) C H N.

7.8 Evaluation of *in vitro* antiplasmodial activity

The *in vitro* antiplasmodial activities of the compounds were evaluated against D10, Dd2 and W2 strains of *P. falciparum*.

The parasites were maintained in continuous *in vitro* culture by standard methods.[38] The cultured parasites were, whenever necessary, synchronized by treatment with 5% D-sorbitol (Sigma) at the ring stage.[39]

For the studies on the D10 and Dd2 strains, the assays were carried out as previously reported by Guantai *et al.* 2010.[16] The assays on the W2 strain were conducted as previously reported (Shenai *et al.* 2003)[40] with parasites cultured in standard medium including 10% human serum, except that parasite development was assessed with a FACS-based assay, as previously described (Sijwali and Rosenthal, 2004).[41] The final concentration of DMSO that the parasites were exposed to did not exceed 0.5%, which has no measurable effect on parasite viability.

7.9 LogD Measurement

Partition coefficient values (LogD) of the test compounds were estimated by correlation of their chromatographic retention properties against the characteristics of a series of standard compounds with known partition coefficient values. The method employed was a gradient HPLC based derivation of the method developed by Lombardo and co-workers, 2001.[29]

7.10 Solubility Estimates

Compound in DMSO was spiked into either pH 6.5 phosphate buffer or 0.01M HCl (approximately pH 2.0) with the final DMSO concentration being 1%. Samples were then analysed via nephelometry to determine a solubility range, as described by Bevan and Lloyd, 2000.[30]

7.11 Evaluation of β-hematin inhibition

β-hematin inhibition assays were conducted as previously reported.[42]

7.12 Evaluation of Falcipain 2 inhibition

Falcipain 2 inhibition assays were carried out as previously described, except that the proteolytic substrate was benzyloxycarbonyl-Phe-Leu-7-amino-4-methyl-coumarin.[43]

7.13 Evaluation of inhibition of sorbitol-induced lysis

The method described by Go *et al.* 2004[36] was applied for this assay, with modifications. Briefly, chloroquine-sensitive *P. falciparum* D10 was cultured and trophozoite-stage infected erythrocytes (10% parasitemia) were harvested by centrifugation (750 r.p.m., 3 min), washed twice with a solution of NaCl (150 mM) – HEPES (20 mM) (pH 7.4; 304

mosM), and suspended in the same solution to give a hematocrit of about 50%. Test compounds were dissolved in dimethylsulfoxide (DMSO) to give 10 mM stock solutions, which were diluted further with a solution comprising 300 mM sorbitol – 20 mM HEPES (pH 7.4; 345 mosM) to give the test solutions of 100 μM.

In 10 mL screw-cap centrifuge tubes, 100 μL of the test solutions were separately combined with an additional 700 μL of the sorbitol-HEPES buffer and 200 μl of the parasitized cell suspension in NaCl-HEPES buffer. The final concentration of the test compounds was 10 μM. For the negative control, 800 μL of the sorbitol-HEPES buffer and 200 μl of the parasitized cell suspension in NaCl-HEPES buffer were transferred into a 10 mL screw-cap centrifuge tube. For the blank, 800 μL of the sorbitol-HEPES buffer and 200 μl of non-parasitized erythrocyte suspension (50% hematocrit) in NaCl-HEPES buffer were transferred into a 10 mL screw-cap centrifuge tube.

The mixtures were incubated at 37°C for 15 min and centrifuged, and aliquots of the supernatant (100 μL) were dispensed into 96-well plates. The absorbances at 560 μm were then determined and used to estimate the amount of hemoglobin released and, by extension, the degree of sorbitol-induced hemolysis. The absorbances of the control and blank wells were determined concurrently, and corrections to the absorbances measured in the test wells were made as appropriate. The percentage inhibition of sorbitol-induced lysis was then calculated for each test compound.

Supplementary Material

Refer to Web version on PubMed Central for supplementary material.

List of abbreviations

ADME	absorption, distribution, metabolism and excretion
DIAD	diisopropyl azadicarboxylate
NADP(H)	Nicotinamide Adenine Dinucleotide Phosphate (reduced)
PK	pharmacokinetic
PPh_3	triphenylphosphine
UDPGA	Uridine Diphosphate Glucuronic Acid
WHO	World Health Organization

Acknowledgments

The authors thank Professor Susan A. Charman of the Centre for Drug Candidate Optimization (CDCO), Monash University (Australia) for kindly facilitating the *in vitro* physicochemical and ADME analysis, and for helpful discussions and assistance with interpretation of the resultant data.

Financial support from the following sources is gratefully acknowledged: the South African National Research Foundation (NRF) by way of the Africa Scholarship (EMG); the South African Research Chair Initiative (SARChI) of the Department of Science and Technology (DST), the South African Medical Research Council (MRC), the University of Cape Town and the European Union through the AntiMal program (KC); the Doris Duke Charitable Foundation and the United States National Institutes of Health (NIH) (PJR).

References

1. WHO World Malaria Report. 2008.
2. WHO Expert Committee on Malaria. WHO Technical Report Series. Twentieth Report. 2000.

3. Price RN, Nosten F. Drug resistant falciparum malaria: clinical consequences and strategies for prevention. Drug Resist. Update. 2001; 4:187–196.
4. WHO Guidelines for the treatment of malaria. 2006.
5. Noedl H, Se Y, Schaener K, Smith BL, Socheat D, Fukuda MM. Evidence of artemisinin-resistant malaria in western Cambodia. New Engl. J. Med. 2008; 359:2619–2620. [PubMed: 19064625]
6. Dondorp AM, Norsten F, Yi P, Das D, Phyo AP, Tarning J, Lwin KM, Ariey F, Hanpithithakpong W, Lee SJ, Ringwald P, Silamut K, Imwong M, Chotivanich K, Lim P, Herdman T, An SS, Yeung S, Singhasivanon P, Day NPJ, Lindegardh N, Socheat D, White NJ. Artemisinin Resistance in *Plasmodium falciparum* Malaria. N. Engl. J. Med. 2009; 361:455–467. [PubMed: 19641202]
7. Ridley RG. Medical need, scientific opportunity and the drive for antimalarial drugs. Nature. 2002; 415:686–693. [PubMed: 11832957]
8. Butina D, Segall MD, Frankcombe K. Predicting ADME properties *in silico*: methods and models. Drug Discov. Today. 2002; 7:S83–S88. [PubMed: 12047885]
9. Yu H, Adedoyin A. ADME-Tox in drug discovery: integration of experimental and computational technologies. Drug Discov. Today. 2003; 8:852–861. [PubMed: 12963322]
10. Shearer T, Smith KS, Diaz D, Asher C, Ramirez J. The role of *in vitro* ADME assays in antimalarial drug discovery and development. Comb. Chem. High T. Scr. 2005; 8:89–98.
11. Smith DA, van de Waterbeemd H. Pharmacokinetics and metabolism in early drug discovery. Curr. Opin. Chem. Biol. 1999; 3:373–378. [PubMed: 10419843]
12. Kerns EH. High throughput physicochemical profiling for drug discovery. J. Pharm. Sci. 2001; 90:1838–1858. [PubMed: 11745742]
13. Ray S, Madrid PB, Catz P, LeValley SE, Furniss MJ, Rausch LL, Guy RK, DeRisi JL, Iyer LV, Green CE, Mirsalis JC. Development of a new generation of 4-aminoquinoline antimalarial compounds using predictive pharmacokinetic and toxicology Models. J. Med. Chem. 2010; 53:3685–3695. [PubMed: 20361799]
14. Kerns, EK.; Di, L. Drug-like Properties: Concepts, Structure, Design and Methods: from ADME to Toxicity Optimization. 1st Ed.. Academic Press/Elselvier; 2008.
15. Masimirembwa CM, Bredberg U, Andersson TB. Metabolic stability for drug discovery and development: Pharmacokinetic and biochemical challenges. Clin. Pharmacokin. 2003; 42:515–528.
16. Guantai EM, Ncokazi K, Egan TJ, Gut J, Rosenthal PJ, Smith PJ, Chibale K. Design, synthesis and *in vitro* antimalarial evaluation of triazole-linked chalcone and dienone hybrid compounds. Bioorg. Med. Chem. 2010; 18:8243–8256. [PubMed: 21044845]
17. Kumar S, Guha M, Choubey V, Maity P, Bandyopadhay U. Antimalarial drugs inhibiting hemozoin (β-hematin) formation: a mechanistic update. Life Sci. 2007; 80:813–828. [PubMed: 17157328]
18. Kunakbaeva Z, Carrasco R, Rozas I. An approximation of the mechanism of inhibition of cysteine proteases: nucleophilic sulphur addition to Michael acceptor type compounds. J. Mol. Struct-Theochem. 2003; 626:209–216.
19. Cruciani G, Crivori P, Carrupt PA, Testa B. Molecular fields in quantitative structure-permeation relationships: the VolSurf approach. J. Mol. Struct-Theochem. 2000; 503:17–30.
20. Cruciani G, Pastor M, Guba W. VolSurf: a new tool for the pharmacokinetic optimization of lead compounds. Eur. J. Pharm. Sci. 2000; 11:S29–S39. [PubMed: 11033425]
21. Boyer D, Bauman JN, Walker DP, Kapinos B, Karki K, Kalgutkar AS. Utility of MetaSite in improving metabolic stability of the neutral indomethacin amide derivative and selective cyclooxygenase-2 inhibitor 2-(1-(4-Chlorobenzoyl)-5-methoxy-2-methyl-1H-indol-3-yl)-N-phenethyl-acetamide. Drug Metab. Dispos. 2009; 37:999–1008. [PubMed: 19196840]
22. Cruciani G, Carosati E, de Boeck B, Erithajulu K, Mackie C, Howe T, Vianello R. Understanding metabolism in human cytochromes from the perspective of the chemist. J. Med. Chem. 2005; 48:6970–6979. [PubMed: 16250655]
23. Milletti F, Storchi L, Sforna G, Cruciani G. New and original pKa prediction method using Grid Molecular Interaction Fields. J. Chem. Inf. Mod. 2007; 47:2172–2181.

24. Gustafsson LL, Walker O, Alván G, Beermann B, Estevez F, Gleisner L, Lindström B, Sjöqvist F. Disposition of Chloroquine in man after single intravenous and oral doses. Brit. J. Clin. Pharmacol. 1983; 15:471–479. [PubMed: 6849784]
25. Winstanley PA, Simooya O, Kofi-Ekue JM, Walker O, Salako LA, Edwards G, Orme ML, Breckenridge AM. The disposition of amodiaquine in man after oral administratrion. Brit. J. Clin. Pharmacol. 1990; 29:695–701. [PubMed: 2378788]
26. Singh T, Stein RG, Hoops JF, Biel JH, Hoya WK, Cruz DR. Antimalarials. 7-chloro-4-(substituted amino)quinolines. J. Med. Chem. 1971; 14:283–286. [PubMed: 5553736]
27. Debaene F, da Silva JA, Pianowski Z, Duran FJ, Winssinger N. Expanding the scope of PNA-encoded libraries: divergent synthesis of libraries targeting cysteine, serine and metalloproteases as well as tyrosine phosphatases. Tetrahedron. 2007; 83:6577–6586.
28. Chipeleme A, Gut J, Rosenthal PJ, Chibale K. Synthesis and biological evaluation of phenolic Mannich bases of benzaldehyde and (thio)semicarbazone derivatives against the cysteine protease falcipain-2 and a chloroquine resistant strain of *Plasmodium falciparum*. Bioorg. Med. Chem. 2007; 15:273–282. [PubMed: 17052908]
29. Lombardo F, Shalaeva MY, Tupper KA, Gao F. $ElogD_{oct}$: A tool for lipophilicity determination in drug discovery. 2. Basic and neutral compounds. J. Med. Chem. 2001; 44:2490–2497. [PubMed: 11448232]
30. Bevan CD, Lloyd RS. A high-throughput screening method for the determination of aqueous drug solubility using laser nephelometry in microtiter plates. Anal. Chem. 2000; 72:1781–1787. [PubMed: 10784141]
31. Weissbuch I, Leiserowitz L. Interplay between malaria, crystalline hemozoin formation, and antimalarial drug action and design. Chem. Rev. 2008; 108:4899–4914. [PubMed: 19006402]
32. Tekwani BL, Walker LA. Targeting hemozoin synthesis pathway for new antimalarial drug discovery: technologies for *in vitro* β-hematin formation assay. Comb. Chem. High Throughput Screening. 2005; 8:63–79.
33. Rosenthal PJ. Cysteine proteases of malaria parasites. Int. J. Epidemiol. 2004; 34:1489–1499.
34. Coterön JM, Catterick D, Castro J, Chaparro MJ, Díaz B, Fernández E, Ferrer S, Gamo FJ, Gordo M, Gut J, de las Heras L, Legac J, Marco M, Miguel J, Muñoz V, Porras E, de la Rosa JC, Ruiz JR, Sandoval E, Ventosa P, Rosenthal PJ, Fiandor JM. Falcipain inhibitors: Optimization studies of the 2-pyrimidinecarbonitrile lead series. J. Med. Chem. 2010; 53:6129–6152. [PubMed: 20672841]
35. Dominguez JN, Charris JE, Lobo G, de Dominguez NG, Moreno MM, Riggione F, Sanchez E, Olson J, Rosenthal PJ. Synthesis of quinolinyl chalcones and evaluation of their antimalarial activity. Eur. J. Med. Chem. 2001; 36:555–560. [PubMed: 11525846]
36. Go ML, Liu M, Wilairat P, Rosenthal PJ, Saliba KJ, Kirk K. Antiplasmodial chalcones inhibit sorbitol-induced hemolysis of *Plasmodium falciparum*-infected erythrocytes. Antimicrob. Agents Chemother. 2004; 48:3241–3245. [PubMed: 15328079]
37. Elderfield RC, Gensler WJ, Birstein O, Kreysa FJ, Maynard JT, Galbreath J. Synthesis of certain simple 4-aminoquinoline derivatives. J. Am. Chem. Soc. 1946; 68:1250–1251. [PubMed: 20990963]
38. Trager W, Jensen JB. Human malaria parasites in continuous culture. Science. 1976; 193:673–675. [PubMed: 781840]
39. Lambros C, Vanderberg JP. Synchronization of *Plasmodium falciparum* erythrocyte stages in culture. J. Parasitol. 1979; 65:418–420. [PubMed: 383936]
40. Shenai BR, Lee BJ, Alvarez-Hernandez A, Chong PY, Emal CD, Neitz RJ, Roush WR, Rosenthal PJ. Structure-activity relationships for inhibition of cysteine protease activity and development of *Plasmodium falciparum* by peptidyl vinyl sulfones. Antimicrob. Agents Chemother. 2003; 47:154–160. [PubMed: 12499184]
41. Sijwali PS, Rosenthal PJ. Gene disruption confirms a critical role for the cysteine protease falcipain-2 in hemoglobin hydrolysis by *Plasmodium falciparum*. Proc. Natl. Acad. Sci. USA. 2004; 101:4384–4389. [PubMed: 15070727]
42. Ncokazi K, Egan T. A colorimetric high-throughput β-hematin inhibition screening assay for use in the search for antimalarial compounds. Anal. Biochem. 2004; 338:306–319. [PubMed: 15745752]

43. Rosenthal PJ, Olson JE, Lee GK, Palmer JT, Klaus JL, Rasnick D. Antimalarial effects of vinyl sulfone cysteine proteinase inhibitors. Antimicrob. Agents Chemother. 1996; 40:1600–1603. [PubMed: 8807047]

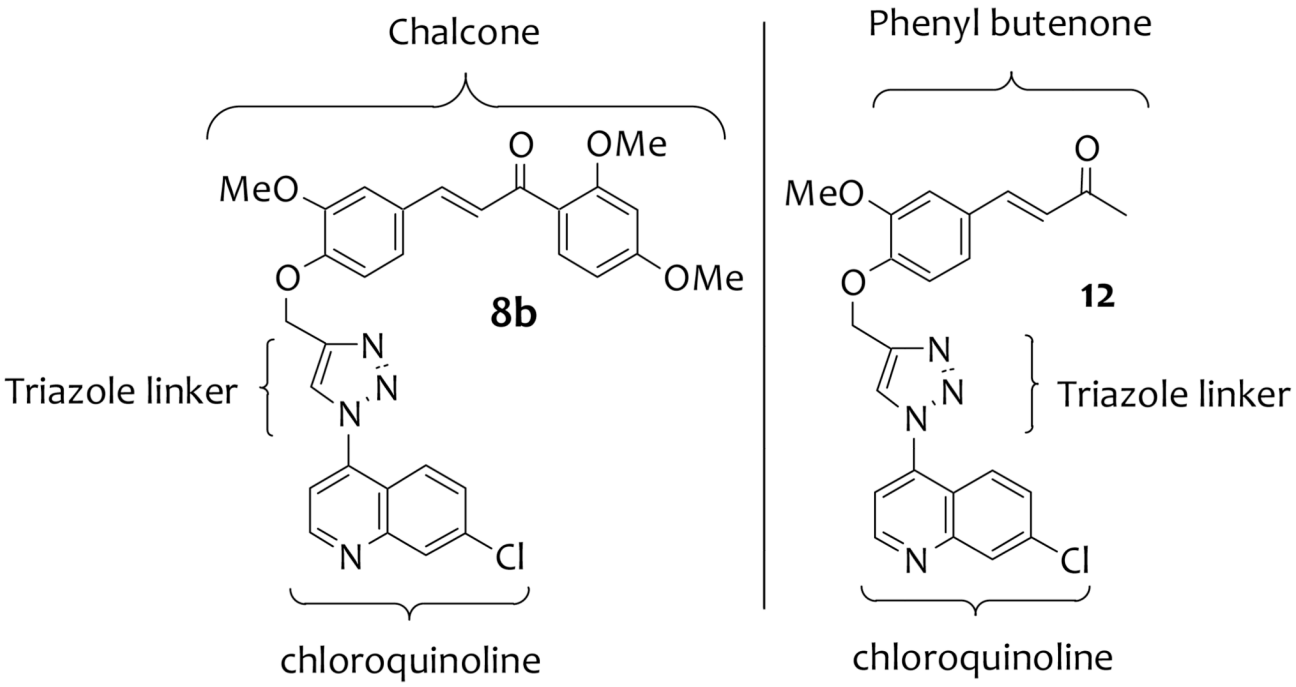

Figure 1.
Core structural features of **8b** and **12**

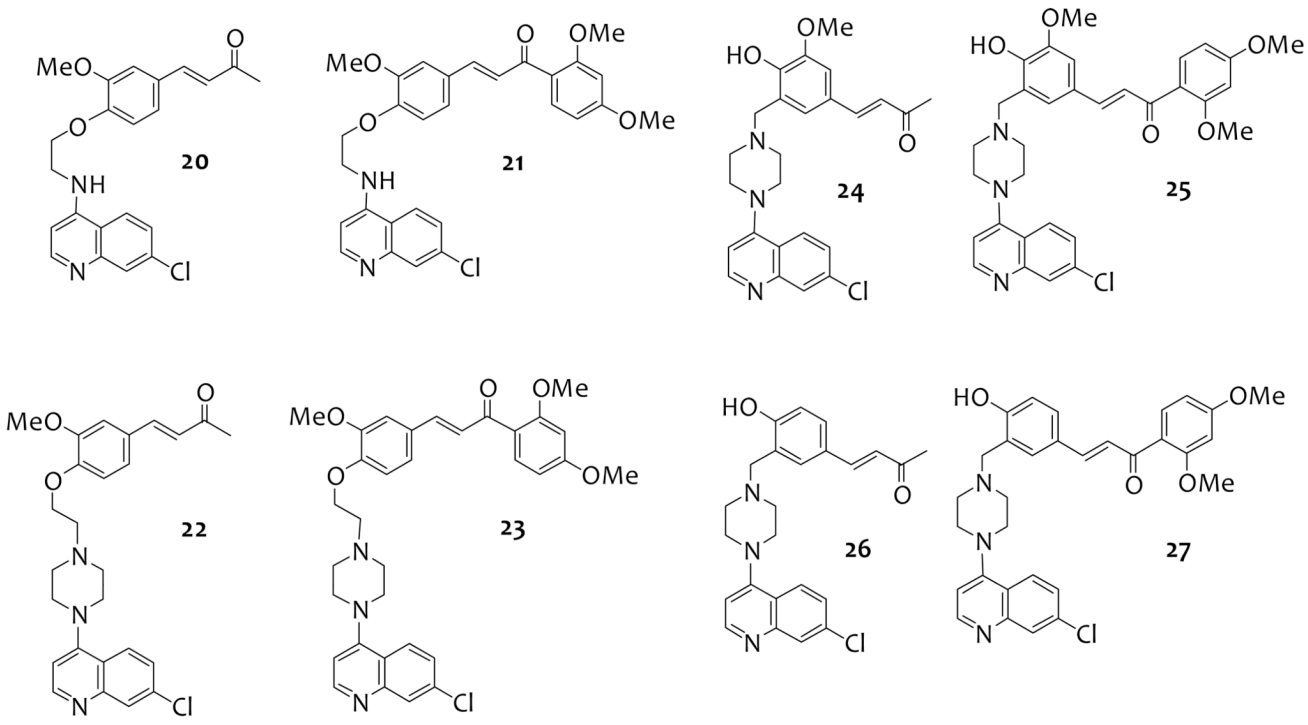

Figure 2.
Structures of analogs of **8b** and **12** derived from replacement of the triazole linker

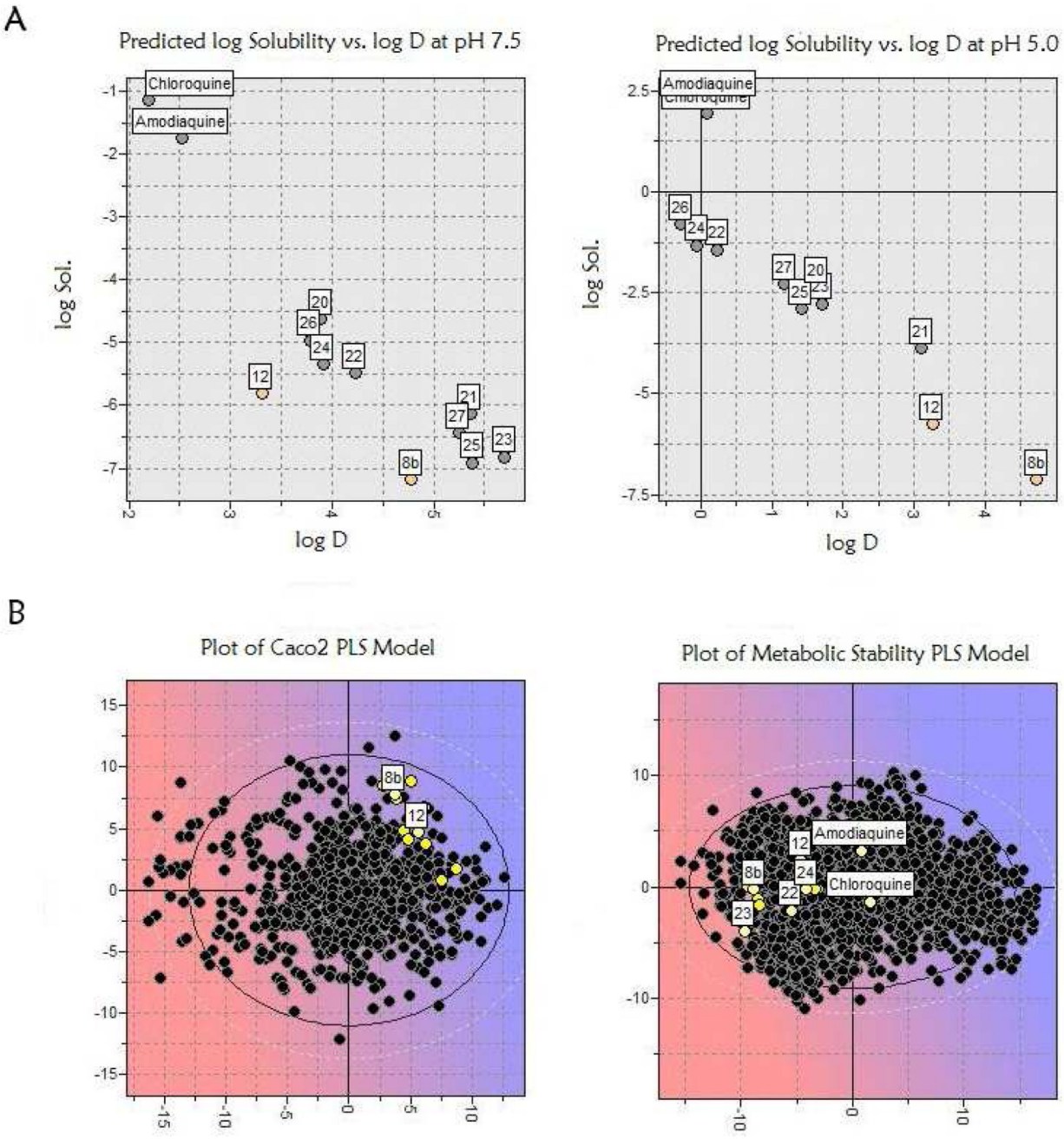

Figure 3.

A: Plots of predicted solubility (expressed as the logarithm, log Sol.) against the predicted n-Octanol-water partition coefficient (also expressed as the logarithm, log D) at pH 5.0 and at pH 7.5; **B:** Plots showing the proposed analogs projected onto the PLS models used to predict Caco2 permeability and metabolic stability – the black dots represent the compounds comprising the models' training data sets while the yellow dots represent the test compounds; the blue regions indicate acceptable predicted permeability/metabolic stability while the red zones indicate poor predicted properties.

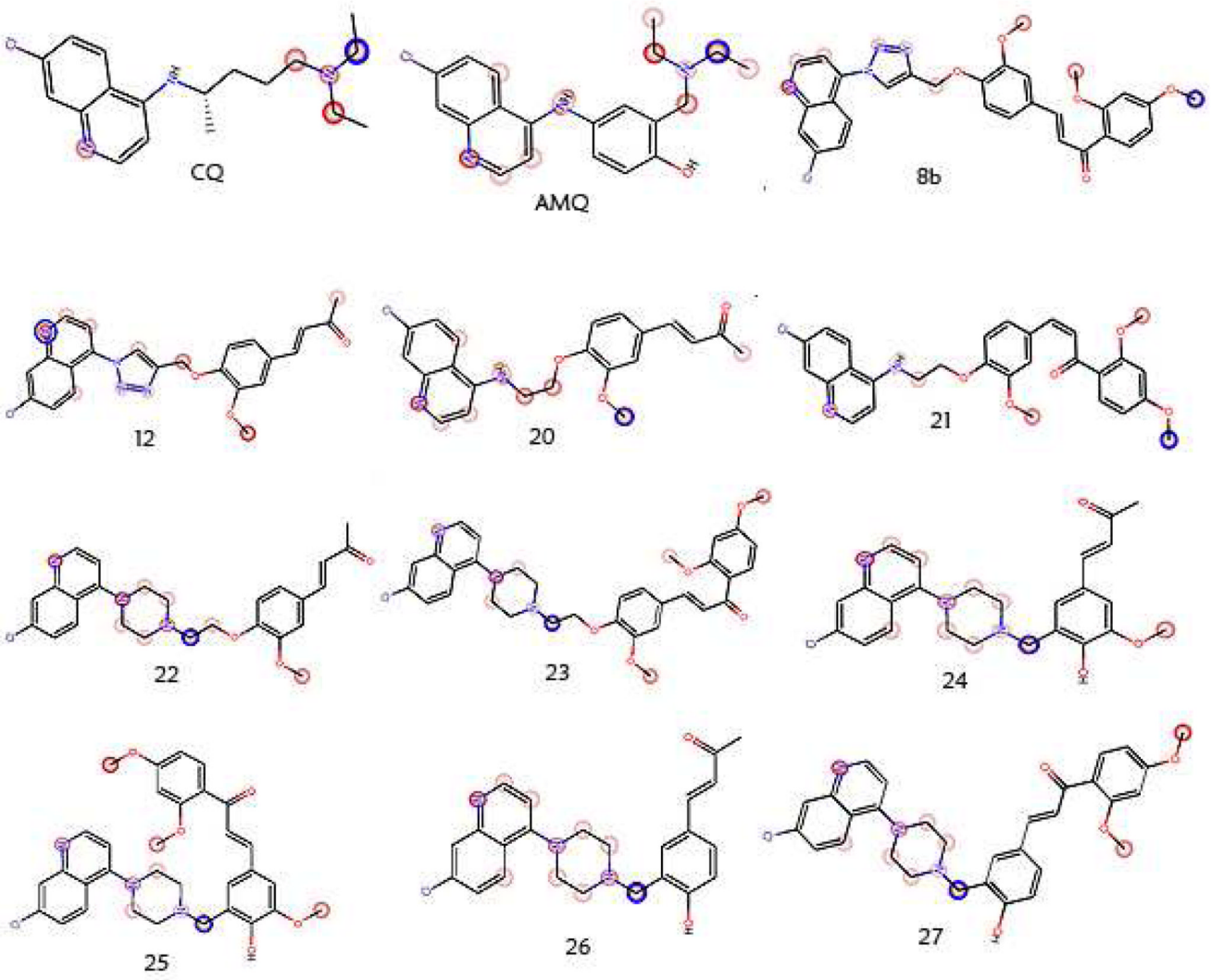

Figure 4.
Output from MetaSite showing the predicted sites of metabolism on the various analogs

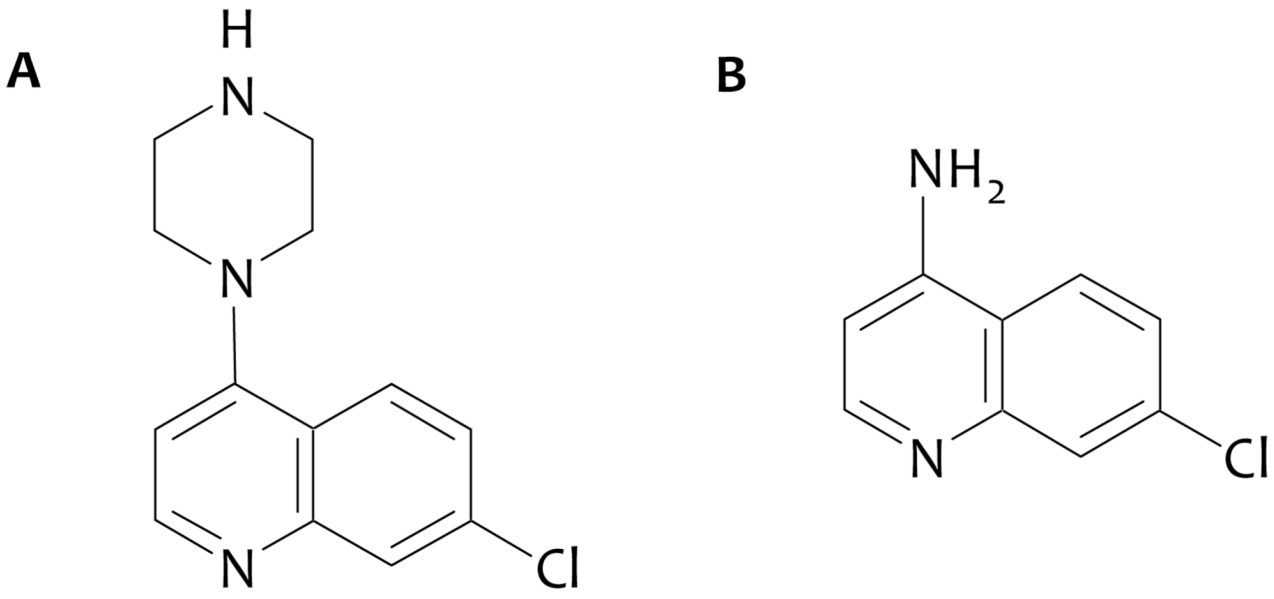

Figure 5.
Figure showing the structures of the putative metabolites of **22 – 27** (**A**) and **20** (**B**)

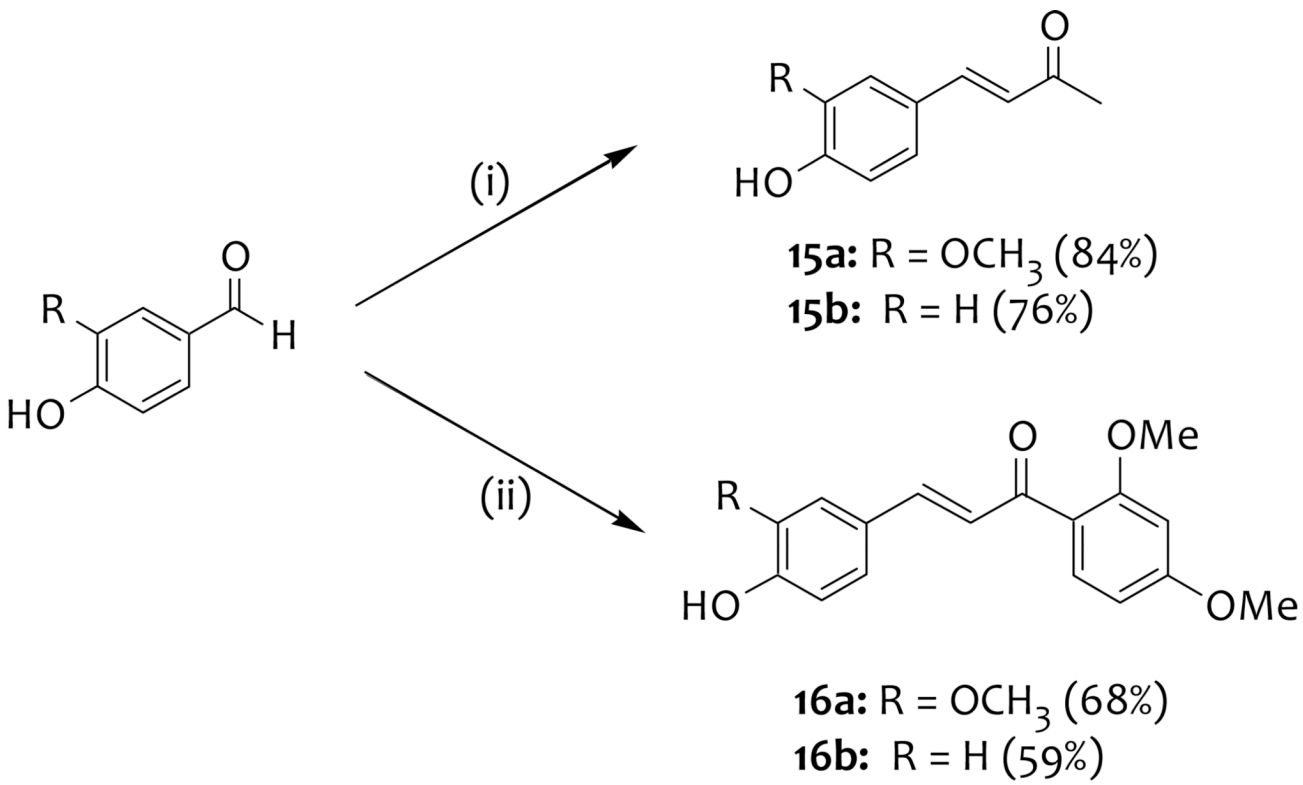

Scheme 1.
Reagents and conditions: (i) acetone, 5M HCl, rt, 24 hrs; (ii) 2',4'-dimethoxy acetophenone, 5M HCl, MeOH, 50 °C, 24 hrs.

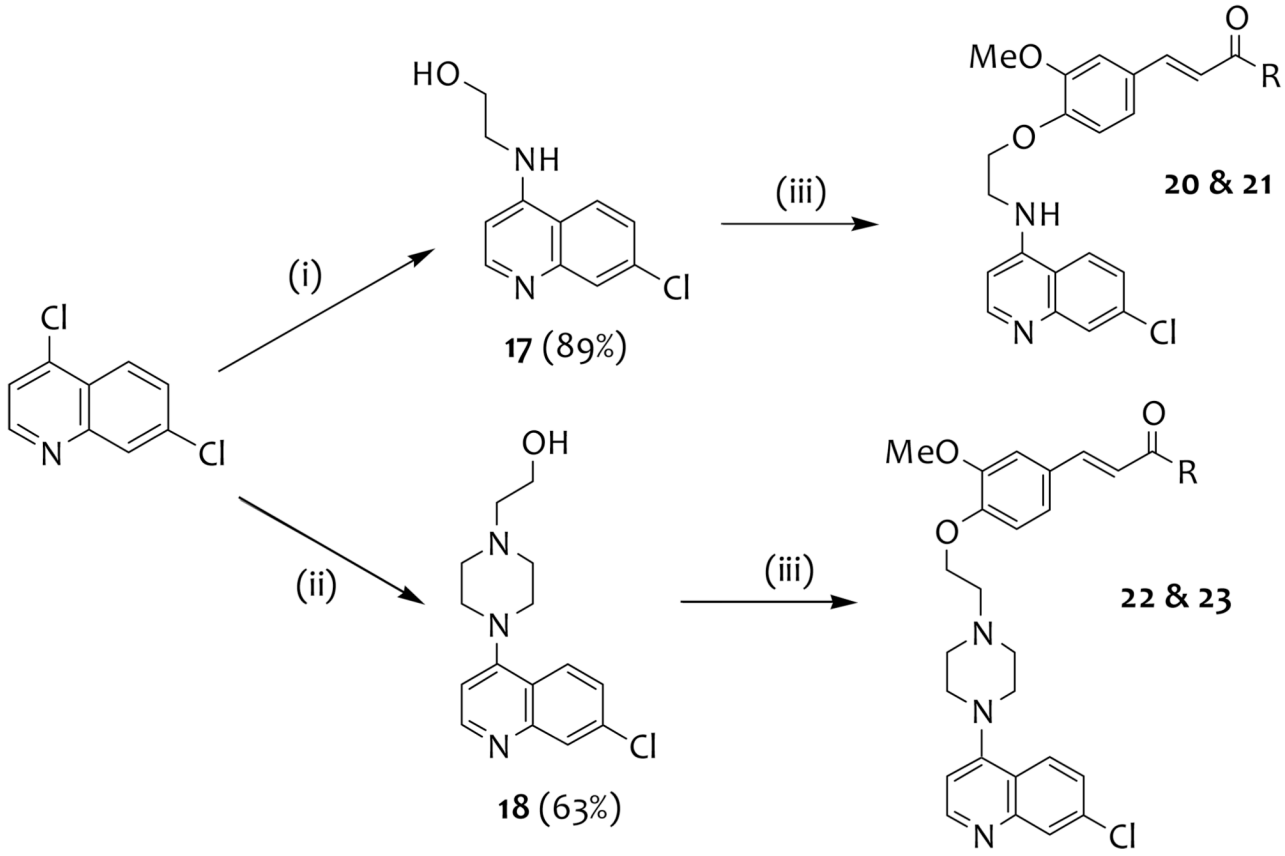

Scheme 2.

Reagents and conditions: (i) ethanolamine, 130 °C, 5 hrs; (ii) 1-(2-hydroxyethyl)piperazine, K_2CO_3, DMF, 80 °C, 24 hrs; (iii) **5.1, 5.2, 5.3** or **5.4**, PPh_3, DIAD, DCM, 0 °C – rt, 6 hrs.

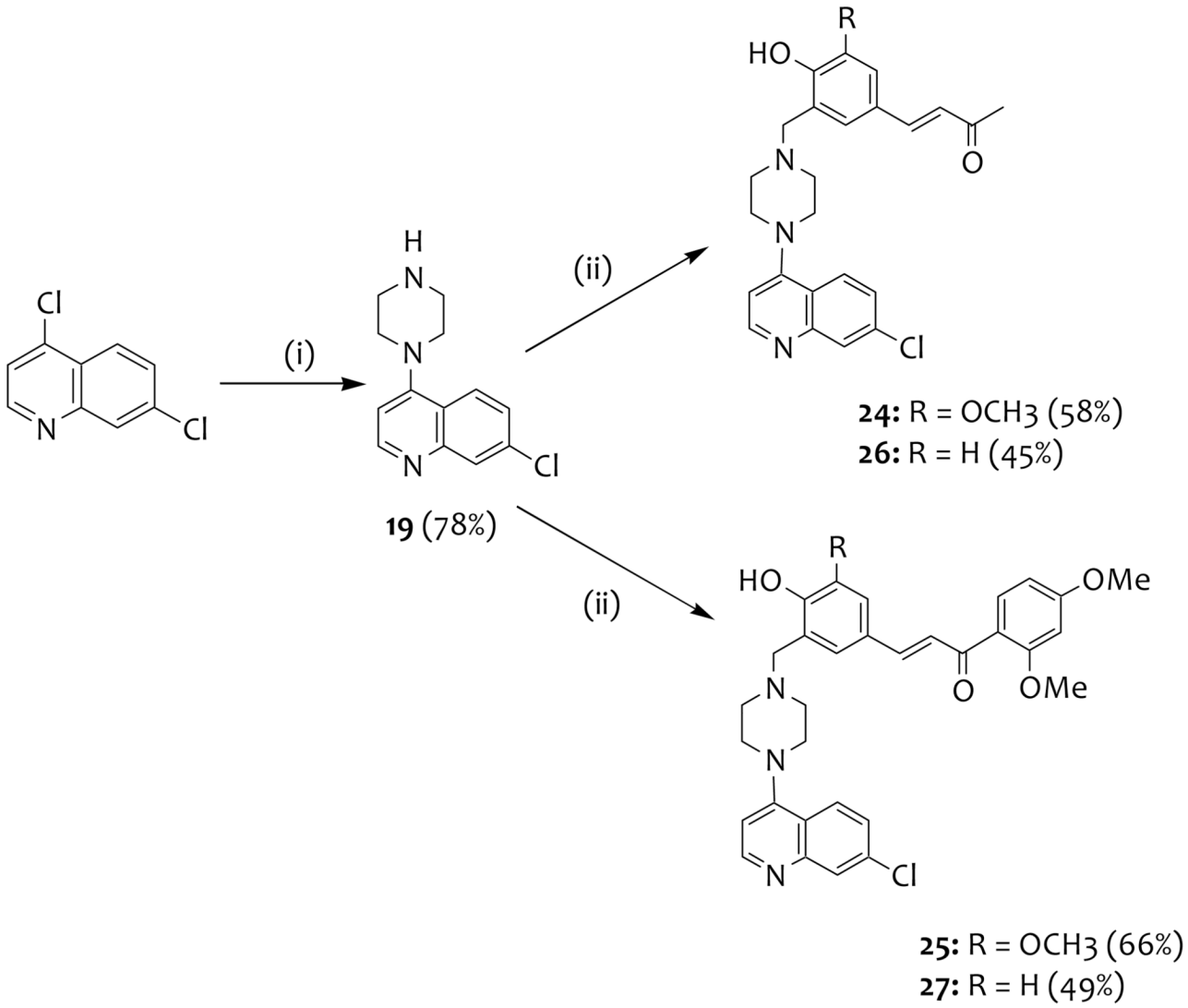

Scheme 3.

Reagents and conditions: (i) piperazine, K_2CO_3, NMP, 135 °C, 4 hrs; (ii) **5.1, 5.2, 5.3** or **5.4**, HCHO, EtOH, reflux at 110 °C, 12 hrs.

Table 1

In vitro antiplasmodial activities against the D10, Dd2 and W2 strains of *P. falciparum* (IC_{50}, μM)

Compound	IC_{50}, μM[a]		
	D10	**Dd2**	**W2**
15a	>20	>20	>10
16a	5.3	7.3	>10
17	2.6	1.0	0.2
18	5.2	3.8	1.0
19	0.7	0.9	0.3
20	1.0	1.5	0.1
21	0.8	1.1	0.4
22	1.2	1.0	0.5
23	1.2	0.5	0.6
24	1.0	1.7	0.5
25	**0.5**	**0.5**	**0.4**
26	1.7	3.1	0.7
27	**0.6**	**0.5**	**0.3**
12	0.8	0.7	ND
8b	0.04	0.07	**0.09**
Chloroquine	0.017	0.097	0.069

[a] average values from two independent determinations, each carried out in duplicate

Table 2

Results from the *in vitro* metabolism studies

Compound		Degradation half-life (min)		Microsome-Predicted Extraction ratio (E_H)		Metabolites detected*
		Human	Mouse	Human	Mouse	
8b		51.1	56.8	0.65	0.57	P+16
12	Peak 1	7.4	10.8	0.93	0.88	Not Detected
	Peak 2	9.1	6.2	0.91	0.92	
20		10.5	13.4	0.90	0.85	P−218
21		17.5	12.7	0.85	0.86	P+16 (x2), P+32 (x2), P−14, P+16+176
22	Peak 1	14.2	6.7	0.87	0.92	P−14, P−218
	Peak 2	9.8	5.6	0.91	0.93	
23	Peak 1	11.5	9.8	0.89	0.89	P+16 (x4), P−14 (x2) P−340
	Peak 2	93.2	149.8	0.51	0.34	
24		16.9	14.0	0.85	0.84	P+16, P−204, P+176 P−14 (x2), P−326, P+176
25		37.0	11.8	0.72	0.87	P+16, P−174, P+176
26		7.5	15.0	0.93	0.84	P+16 (x2), P−14, P−296 P+176
27		58.6	45.4	0.62	0.63	
Chloroquine		>250	177.0	<0.28	0.31	Not Undertaken

* as represented by fragments detected after Mass Spectroscopy analysis, and which had m/z values corresponding to putative metabolites; P represents the molecular mass of the parent compound; the interpretation of the results is contained in-text in the section ‘Putative Metabolite Identification’.

J Med Chem. Author manuscript; available in PMC 2012 May 26.

Table 3

Results from the experimental determination of solubility and partition coefficients

Compound	LogD[a]		Solubility (μg/mL)	
	pH 3.0	pH 7.4	pH 2.0	pH 6.5
8b	4.3	4.3	< 1.6	< 1.6
12	3.5	3.6	3.1 – 6.3	3.1 – 6.3
20	1.8	3.0	50.0 – 100.0	6.3 – 12.5
21	2.8	4.2	> 100	3.1 – 6.3
22	1.2	4.2	> 100	1.6 – 3.1
23	2.2	5.3	> 100	< 1.6
24	0.9	3.9	> 100	1.6 – 3.1
25	2.1	5.0	> 100	< 1.6
26	0.8	4.2	> 100	< 1.6
27	2.0	5.3	> 100	< 1.6
Chloroquine	0.4	2.0	> 100[b]	>100[b]

[a] Value measured using the chromatographic gLogD technique.

[b] Stock solution of compound prepared in water at 10 mg/mL concentration

Table 4

Results from the mechanistic studies

Compd	β-hematin formation (IC_{50})[a]	Falcipain 2 (IC_{50};μM)[b]	Inhibition of sorbitol-induced hemolysis (%)[c]
15a	>5	>50	21.1
15b	>5	>50	ND
16a	>5	>50	27.9
16b	1.9	>50	ND
17	4.9	>50	0.9
18	3.9	>50	ND
19	>5	>50	5.8
20	0.6	>50	12.3
21	0.3	22.9	ND
22	0.5	>50	ND
23	0.2	11.7	ND
24	0.5	>50	16.8
25	0.3	9.1	3.9
26	0.5	29.9	11.6
27	0.2	10.0	ND
8b	1.6	10.8	15.4
Chloroquine	1.91	-	-
E64	-	0.055	-

[a] The IC_{50}s are averages of triplicate determinations and are reported as equivalents of the compound (relative to hematin) that inhibit the formation of β-hematin by 50%.

[b] Averages of duplicate determinations.

[c] Inhibition of sorbitol-induced lysis at a concentration of 10 μM.

ND: Not determined